ELSEVIER

Journal of Environmental Management 78 (2006) 63–76

Journal of Environmental Management

www.elsevier.com/locate/jenvman

Identifying hydrologically sensitive areas: Bridging the gap between science and application

Laura J. Agnew[a], Steve Lyon[a], Pierre Gérard-Marchant[a], Virginia B. Collins[a], Arthur J. Lembo[b], Tammo S. Steenhuis[a], M. Todd Walter[a,*]

[a]*Department of Biological and Environmental Engineering, Cornell University, Ithaca, NY 14853-5701, USA*
[b]*Department of Crop and Soil Sciences, Cornell University, Ithaca, NY 14853, USA*

Received 24 September 2004; revised 19 March 2005; accepted 8 April 2005
Available online 19 September 2005

Abstract

Researchers have noted that current water quality protection strategies, like nutrient management plans, lack a sound hydrological underpinning for pollutant transport processes. This is especially true for areas like the northeastern U.S. where copious research has shown that variable source area hydrology largely governs runoff generation. The goal of this study was to develop a scientifically justified method to identify the locations that generate overland flow. Furthermore, this methodology must be computationally simple enough that it can be utilized or incorporated into nutrient management plans and other established water quality tools. We specifically tested the reliability of the 'distance from a stream,' D_s, and the 'topographic index,' λ, to predict areas with a high propensity for generating overland flow, i.e. hydrologically sensitive areas (HSA). HSAs were defined by their probability of generating runoff, P_{sat}, based on 30 year simulations using a physically based hydrological model. Using GIS, each location's P_{sat} was correlated with D_s and λ. We used three Delaware Co., NY watersheds in the New York City watershed system with areas varying in size from 1.6 to 37 km^2 and with forested and agricultural land uses. The topographic index gave stronger, more regionally consistent correlations with P_{sat} than did D_s. Equations correlating λ and P_{sat} for each month are presented and can be used to estimate hydrological sensitivity in the region surrounding our study watersheds, i.e. in Delaware Co. This work is currently being incorporated into an Internet Mapping System to facilitate user-friendly, on-line identification of HSAs.

Keywords: Hydrologically sensitive areas (HSA); Water quality; Nonpoint Source (NPS) pollution; Variable source area (VSA) hydrology; Topographic index; Soil moisture routing model (SMR)

1. Introduction

Amendments to the Clean Water Act (1972), especially those in 1987, increasingly emphasized nonpoint source (NPS) pollution as a critical cause of water quality degradation (Segars, 1997). Since, agriculture covers a major portion of the landscape in many parts of the country, there is particular concern about NPS pollution from farms. Overland flow, or runoff, is a primary hydrological vector for potential agricultural pollutants although the implementation of current management practices, like conservation buffers, does not utilize up-to-date scientific understanding of how runoff is generated.

In fact, agricultural practices and management strategies for reducing NPS pollution are generally lagging the scientific state-of-the-art by several decades (Walter et al., 2000). Many current attempts to reduce NPS pollution of surface water bodies primarily utilized the typical, traditional suite of soil and water conservation practices developed in the 1930s, i.e. the dustbowl days, to combat soil erosion and increase water retention in the soil (Walter et al., 1979). These practices do not result in the expected reductions in pollution in part because they fail to address the transport processes of dissolved nutrients, especially dissolved phosphorus (P), which are directly linked to eutrophication. (e.g. Brannan et al., 2000; Inamdar et al., 2001). A new set of tools that are in accordance with the current hydrological science are needed to guide better management decisions thereby reducing the impact of

* Corresponding author. Tel.: +1 607 255 2488; fax: +1 607 255 4080.
E-mail address: mtw5@cornell.edu (M.T. Walter).

0301-4797/$ - see front matter © 2005 Elsevier Ltd. All rights reserved.
doi:10.1016/j.jenvman.2005.04.021

nutrients and other agricultural chemicals on receiving water bodies.

Undoubtedly, developing water quality management tools consistent with contemporary scientific understanding of the hydrologic processes involved in pollutant transport will likely lead to improved water quality protection strategies. Two interconnected hydrological-water quality concepts that are useful are hydrologically sensitive areas (HSAs) and critical source areas (CSAs). An HSA is any area in a watershed that is prone to generating runoff and therefore has the potential to transport pollutants (Walter et al., 2000). A CSA is an area in a watershed where potential pollutant loading coincides with an HSA. Recently published work on HSAs and CSAs has shown that adopting these concepts into farm management has good potential to substantially reduce NPS P-loading associated with dairy manure spreading (e.g. Gburek and Sharpley, 1998; Walter et al., 2001; Gburek et al., 2002; Hively, 2004). However, the primary unresolved challenge to developing HSA/CSA-based agricultural management practices is finding cost-effective, user-friendly ways of identifying HSAs; indeed, this study proposes some ideas for addressing this challenge. A prerequisite to HSA identification is an understanding of what hydrological processes are generating runoff.

There are two primary runoff (overland flow) mechanisms, infiltration excess overland flow and saturation excess overland flow. Infiltration excess overland flow, also commonly called Hortonian flow in recognition of Robert Horton's early contributions to our understanding of this process, occurs when precipitation intensity is greater than the soil's infiltration capacity (e.g. Horton, 1933, 1940). In contrast, saturation excess overland flow occurs when the soil's capacity to store water is exceeded and additional water that enters the saturated area runs off as overland flow (e.g. Hursh, 1944; Dunne, 1970). Hortonian flow most commonly occurs during very high intensity rain storms and in areas where the ground's infiltration capacity is particularly low, which may be attributed to the soil's natural or modified structure, compaction processes, and/or surface sealing, especially where there is too little vegetation to protect the soil surface from raindrop impact. Saturation excess is mostly common in humid, well-vegetated regions (e.g. Dunne and Black, 1978 pp. 273) where soil infiltration capacities are high and soils are shallow or the water table is high, so the soil is especially prone to saturate (e.g. Hewlett and Hibbert, 1967; Dunne and Black, 1970). The variable source area (VSA) hydrology concept notes that the size of runoff generating saturated areas will vary over time with landscape wetness, on temporal scales ranging from a single storm to seasonal fluctuations (e.g. Dunne and Black, 1970; Hewlett and Nutter, 1970; Dunne et al., 1975). Note that VSAs are a physical, scientific concept whereas HSAs are a water quality concept that describes the risk of runoff generation.

Current water quality protection decisions are often made based on results from models like SWAT (Arnold et al., 1983), AGNPS (Young et al., 1989), and GWLF (Haith and Shoemaker, 1987) that are based on the antiquated SCS-Curve Number rainfall-runoff equation (e.g. USDA-SCS, 1972). The SCS-Curve Number is officially parameterized by soil type and land use, both of which are associated with infiltration capacity, thus, implying Hortonian runoff. Note that the SCS-Curve Number equation was developed as an engineering tool for estimating design storm flows (Rallison, 1980; Tollner, 2002; USDA-SCS, 1986) and not for predicting pollutant transport, which can be substantial even at low flow rates. Perhaps the most severe shortcoming of current water quality models like SWAT, AGNPS, and GWLF is that they are evaluated based on their ability to correctly predict storm flow hydrographs with no attention to the locations of runoff producing areas, which is central to identifying HSAs (Rossing and Walter, 1995). In areas where saturation excess overland flow is more prevalent then Hortonian flow, these models are obviously inappropriate most of the time (Walter et al., 2003). Additionally, they typically assume that the hydrological response of individual points in the landscape is independent of the hydrology of the surrounding area, which is generally a poor assumption for both runoff mechanisms.

New water quality models are needed that preserve the geographically distributed information and capture VSA hydrological processes so that HSAs associated with saturated areas in the landscape can be identified. Although there has recently been several physically based distributed hydrological models that consider VSA hydrology, as with many of the current water quality models mentioned earlier, most require large amounts of input data and/or substantial calibration (e.g. Bernier, 1985; Beven, 1989; Wigmosta et al., 1994), which makes application to ungaged watersheds uncertain (Grayson et al., 1992; Beven, 2000). TOPMODEL (e.g. Beven and Kirkby, 1979) and its copious variations, and the Soil Moisture Routing model (SMR) (e.g. Zollweg et al., 1996; Kuo et al., 1996; Frankenberger et al., 1999), and its derivatives, are two parsimonious VSA hydrological modeling concepts that have strong potential for future water quality modeling. Both models have been shown to successfully identify saturated areas albeit for somewhat different types of systems (e.g. for SMR, Mehta et al., 2004; for TOPMODEL, Holko and Lepisto, 1997). TOPMODEL is based on the assumption that a watershed-wide water table intersects the landscape to produce saturated runoff generating areas and SMR assumes that these areas are controlled by transient interflow perched on a shallow restricting layer. TOPMODEL is based on a steady-state assumption and requires some calibration and SMR, which is based on a simple physically-based water budget, requires virtually none.

Although more physically realistic NPS pollution models are inevitable, in the short-term there is an immediate need for better strategies for water quality protection based on our current knowledge. With respect to the northeastern U.S. this means new tools to predict the locations and timing of

HSAs. Gburek et al. (2002) proposed one such tool based on Curve Numbers and the assumption that saturated areas concentrate around perennial waterways. In this paper, we propose alternative approaches to identifying HSAs that we feel are based on a more physically robust description of VSA hydrology. One objective is that the HSA tool developed be simple enough that it can be implemented through the Internet, and thus be rapidly available to a wide range of users. We test our HSA identification approaches in the Catskills region of New York State and discuss the weaknesses and strengths of each.

2. Description of a new HSA identification method

We assumed that within a region characterized by homogeneous climate, geology, and topographic characteristics, the patterns of VSA hydrology would also be similarly homogeneous. Thus, if we can develop relationships for identifying HSAs that are consistent for a small subset of 'test' watersheds, the guidelines should be applicable across the region as a whole. The more consistent a guideline is among the test watersheds, the more confident we are that the guidelines will be applicable to the region as a whole.

HSAs can be characterized by the probability that a particular location in a watershed will generate runoff (e.g. Walter et al., 2000). To capture seasonal variability in HSAs, we recommend determining their spatial distribution for each month (e.g. Walter et al., 2001). While either direct or remotely sensed data would provide the most accurate measures of runoff generation, these data are generally not available for long enough periods or large enough areas to calculate a reliable 'probability' of runoff generation. In lieu of direct measurements, an appropriate physically-based model must be used to simulate distributed runoff over a long period of time, e.g. 30 years. For example, SMR has been shown to accurately predict the location and timing of saturated areas in the Catskill Mountain region of New York State (e.g. Frankenberger et al., 1999; Mehta et al. 2004), and would, therefore, be an obvious model choice for this region. Different models may better describe the hydrology of other areas.

The two HSA indices or proxy-parameters we propose correlating to HSAs are (1) a topographic index, λ, and (2) proximity to a stream, D_s. Both of these proxy-parameters are easy to calculate, are based on static, easily measured characteristics, and have been linked to descriptions of VSA hydrology. For example, topographic indices have been associated with VSA hydrology by, among others, Beven and Kirkby (1979) and O'Loughlin (1986). Stream proximity was used as a VSA proxy by Gburek et al. (2002). We anticipate that other HSA proxy-parameters will emerge with time. Fig. 1 is a schematic of the general methodology we are proposing.

The topographic index we use is similar to expressions used previously (e.g. Sivapalan et al., 1987; Ambroise et al., 1996; Lyon et al., 2004):

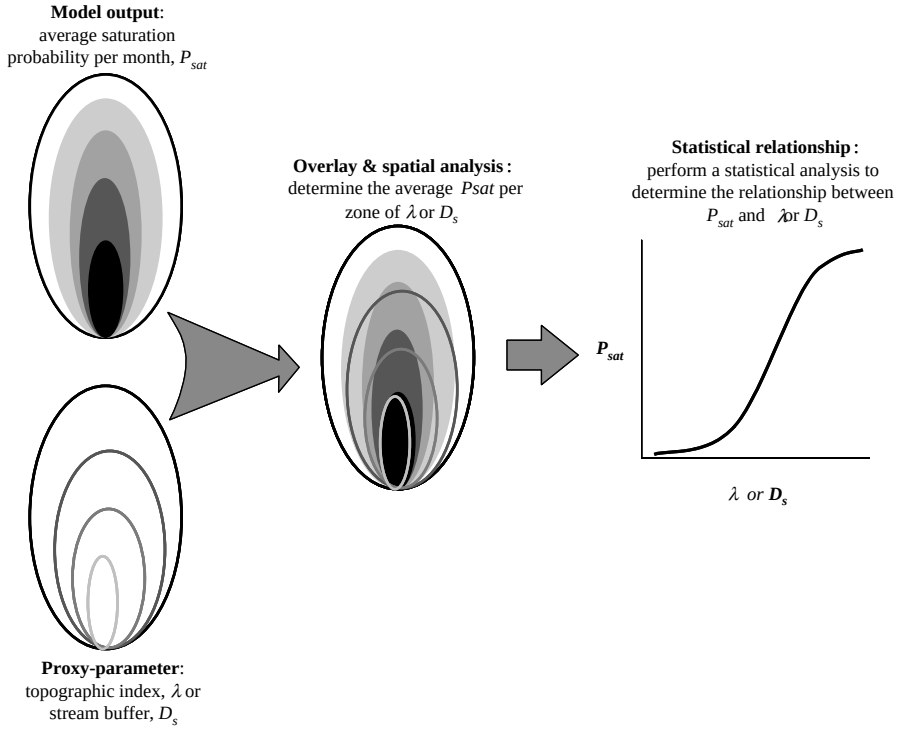

Fig. 1. Schematic of the methodology used to combine output from a mechanistic hydrology model with a proxy index to develop a simple relationship for identifying HSAs.

$$\lambda = \ln\left(\frac{a}{\tan(\beta)K_s D}\right) \quad (1)$$

where λ is the topographic index [units of $\ln(\mathrm{d\,m^{-1}})$], a upslope contributing area per unit contour length (m), $\tan(\beta)$ is the local surface topographic slope, K_s is the mean saturated hydraulic conductivity of the soil ($\mathrm{m\,d^{-1}}$), and D is the soil depth (m). This topographic index can be easily determined for every point in the landscape using a geographic information system (GIS) and requires a digital elevation model (DEM) and soils data such as those in SURRGO or STATSGO.

The stream proximity or 'distance from stream,' D_s, can also be determined in a GIS by developing a map of 'buffers' around the stream system. Stream proximity is quantified as the shortest distance to the stream and obviously requires very few data and has the advantage over the topographic index in that it can be easily determined in the field.

HSA relationships are developed by correlating a proxy-parameter to monthly estimates of hydrological sensitivity as determined by a distributed hydrological model such as SMR and a local meteorological record, which is readily available via the National Climate Data Center (NCDC). The result is twelve monthly relationships of hydrological sensitivity, i.e. runoff generating probability, as a function of the proxy-parameter. Fig. 1 is a schematic diagram describing our methodology for developing HSA relationships. These relationships can then be used to estimate hydrological sensitivity for regional watersheds via the appropriate proxy-parameter.

3. Application to Delaware County, New York

We chose three well-monitored, stream-gauged watersheds of varying sizes and land uses as our representative subset of Delaware County test watersheds (Fig. 2). All are sub-watersheds of the New York City watershed system located in New York's Catskill Mountains. Monthly HSAs were calculated for each watershed with SMR using 36 years of data (1960–1996). The topographic index and stream proximity were calculated for each watershed and correlated to the modeled monthly HSAs. The correlations

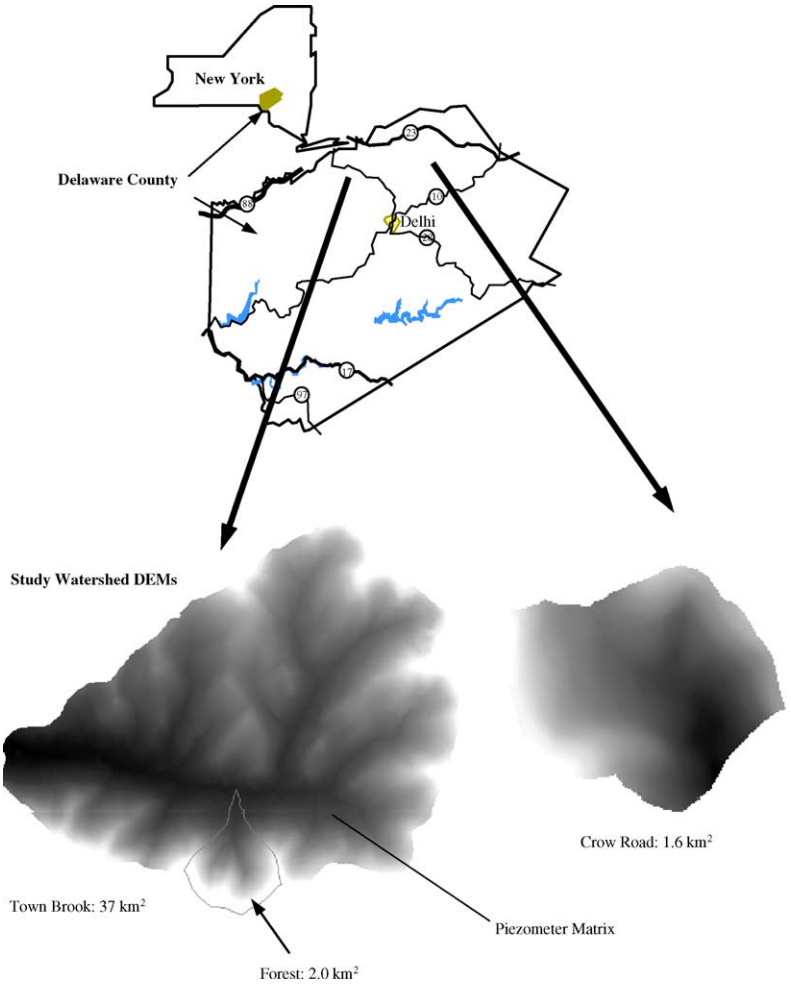

Fig. 2. Locations of Delaware County, NY and the study watersheds. The watersheds are shown as digital elevation models (DEM) with dark regions corresponding to low elevations. Circle shows the location of piezometer matrix.

for each watershed were compared to each other to evaluate regional consistency.

3.1. Descriptions of test watersheds

The Crow Road watershed has an area of 1.6-km^2 with an elevation range of 600–739 m (Fig. 2). In the upper part of the watershed, shallow (average thickness 65 cm) soil overlays fractured bedrock and the terrain is steep (average slope 18%). At lower elevations, deeper soils (average thickness 180 cm) overlay a dense fragipan and the topography is flatter (average slope 10%). Approximately 53% of the watershed is covered by deciduous forest. The lower slopes consist of improved and unimproved pastures (38%), rotated crops (7%) and impervious areas such as roads and buildings (2%).

The Town Brook watershed is the largest watershed of the three, with an area of 37-km^2 and an elevation range of 493–989 m (Fig. 2). Shallow soil (average thickness 80 cm) overlaying fractured bedrock, steep slopes (average slope 29%), and deciduous and mixed forests (about 49% of the watershed area) characterize the upper terrain of the watershed. The lower portions of the watershed have deeper soils (average thickness 180 cm) overlaying a dense fragipan, are flatter (average slope 14%), and are covered by shrubs, pastures and rotating crops (31%, 17% and 2% of the watershed area respectively). A 2.44 ha matrix of automated, continuously monitoring piezometers (Tru-Track, Inc., WT-HR 500 capacitance probes) was instrumented for about 100 m along a first-order stream (Fig. 2). The piezometers were used to get a direct measure of saturation frequency to compare against our proxy-parameters of saturation; at the time of this paper, data were only available for March–August 2004. For more details about the field measurements, see Lyon et al. (2005).

The forested watershed is a 2-km^2 sub-basin of the Town Brook watershed (Fig. 2). The elevation ranges from 554 to 984 m and slopes range from 0 to 84%. The primary land cover is deciduous forest (93%) with small amounts of open grassed areas (7%). The location of the forested sub-basin within the Town Brook watershed is shown in Fig. 2. Ideally we would have preferred a forested watershed completely independent of the other two basins but there were no others available with stream gages and an on-going monitoring program.

3.2. Saturation probability (HSA) determination, P_{sat}

Distributed risk or probability of saturation was determined on a monthly basis for each of the watersheds using SMR in GRASS version 5 (U.S. Army CERL, 1991).

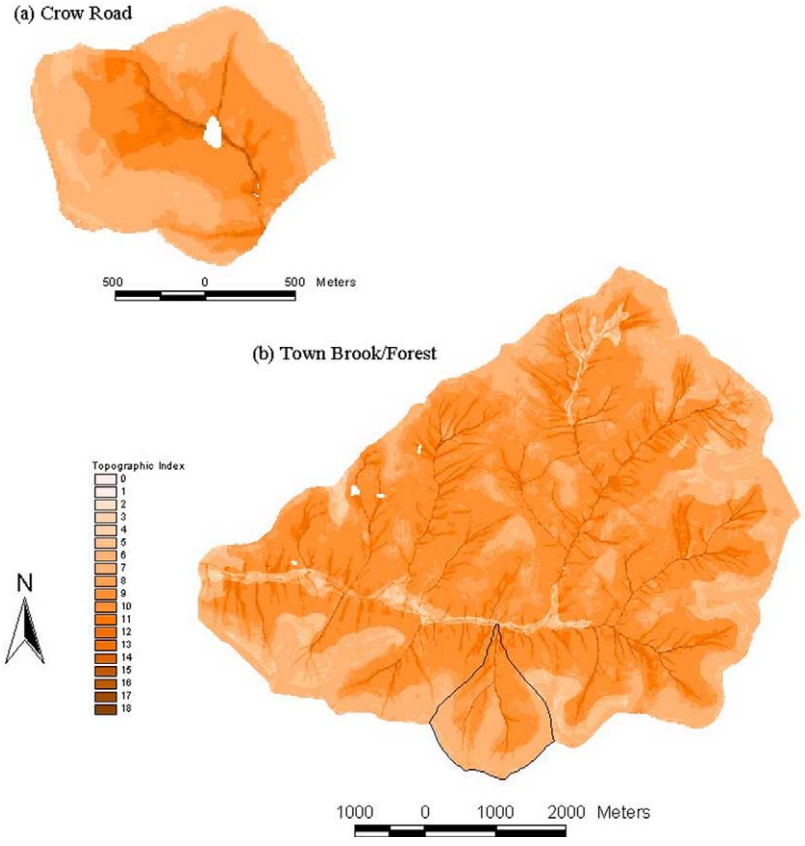

Fig. 3. The topographic index (λ) maps for the (a) Crow Road and (b) Town Brook and Forested watersheds. The white areas are ponds and were not included in the analysis.

SMR is a spatially distributed hydrological modeling concept that calculates a daily water balance on a cell-by-cell basis and routes water through the watershed to the outlet (e.g. Zollweg et al., 1996; Kuo et al., 1996; Frankenberger et al., 1999). SMR predicts distributed soil moisture in the test watersheds. A complete description and evaluation of SMR is available at the Cornell Soil and Water Lab website (SWL website). The inputs needed for this model include a DEM, basic meteorological data, and soils data. SMR estimated daily saturated areas from 08/1960 to 05/1996 using a USGS 10-m DEM, Northeast Regional Climate Center weather data, and SURRGO soil data. The daily model results were condensed to monthly saturation probability, P_{sat}, by tallying the number of days that a cell in the raster data set is saturated and dividing by the total number of simulated days in that month (Walter et al., 2000).

3.3. Topographic index determination, λ

The topographic index, λ, was calculated using Eq. 1, following the multidirectional flowpath algorithm of Quinn et al. (1991). The upslope area and slope were derived from 10-m USGS DEMs and the soil depth and saturated hydraulic conductivity were obtained from SSURGO data. The topographic index maps for the Crow Road, Town Brook, and forested watersheds are shown in Fig. 3.

3.4. Stream proximity determination, D_s

The GRASS GIS was used to create buffers, D_s, around the topographically-based stream in 10-meter increments (Fig. 4a, b). The New York City Department of Environmental Protection provided GIS stream coverages. The Crow Road stream coverage was modified to coincide with the most recent DEM (1998) and field observations of human modifications to the stream network that were unaccounted for in the original stream coverage.

3.5. HSA relationship with proxy parameters

The topographic index and stream buffer coverages or maps for each watershed were overlaid on the respective monthly saturation probability maps using a zonal statistics function in ESRI's ArcGIS 8.2™. This function provided the average saturation probability, P_{sat}, per zone of topographic index, λ, or stream buffer, D_s. We used integer values of λ to delineate our topographic index zones. For the D_s, we divided the zones by 1 m increments. The resulting database files were statistically analyzed both on an individual watershed basis and with all three watersheds combined to determine the relationship between average saturation probability and topographic index or stream buffer for each month of the year.

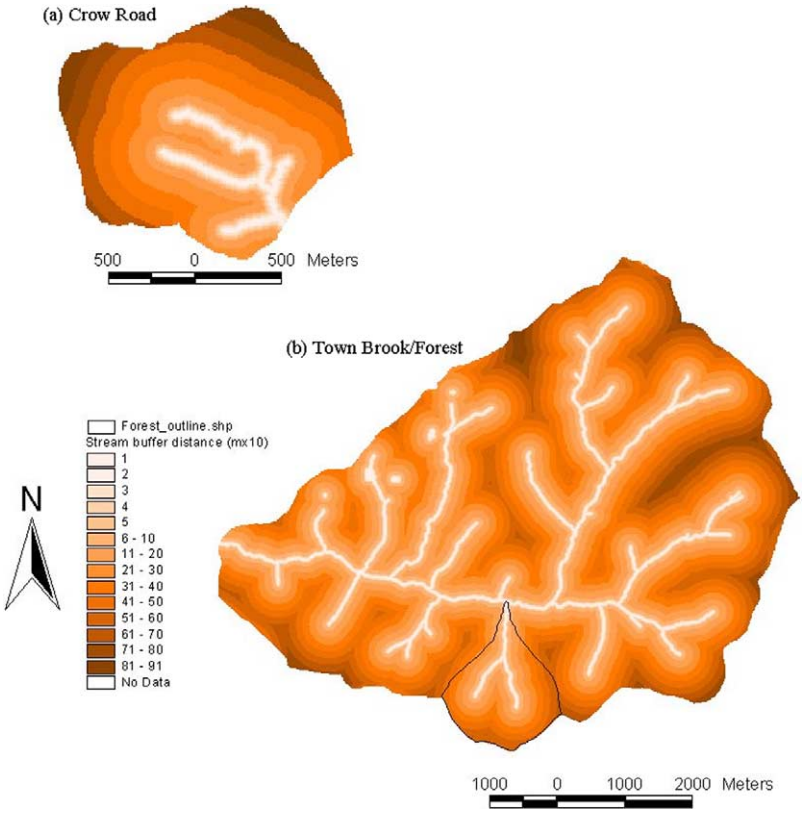

Fig. 4. The stream buffer, or stream proximity, maps for the (a) Crow Road and (b) Town Brook and Forested watersheds.

4. Results

4.1. Modeled probability of runoff generation

SMR reproduced soil moisture distributions in the watersheds landscape well (Fig. 5), relative differences between observed and simulated soil moisture were consistently $<10\%$. For more information about SMR evaluation see Frankenberger et al. (1999), Mehta et al. (2004), or the Cornell Soil and Water Lab website (SWL website). Given the good agreement between measured and observed soil moisture, saturation probability maps for the watersheds are considered good estimates of the distributions of average P_{sat} (Fig. 6). Throughout the remainder of this paper we will use April, August, and October (e.g. Fig. 6a,b,c, respectively) as representative of spring, summer, and fall conditions, respectively in order to illustrate seasonal variations according to the VSA concept. As expected, wetter months, i.e. April and October, which have low evapotranspiration (ET), have larger areas with high probability of saturation, P_{sat}, than the dry summer months, i.e. August (Fig. 6). Also, the areas that are most prone to saturation, i.e prone to generating saturation excess runoff, are consistently in the low-lying or flat parts of the watershed. No water quality models or BMPs currently account for this type of dynamic behavior in hydrological sensitivity.

4.2. Topographic index results

For each month, April, August, and October, the P_{sat}–λ relationship was similar for all three watersheds (Fig. 7); in particular, note the values of λ where the regression line intercepts $P_{sat}=0$ and $P_{sat}=100\%$, which we will refer to as

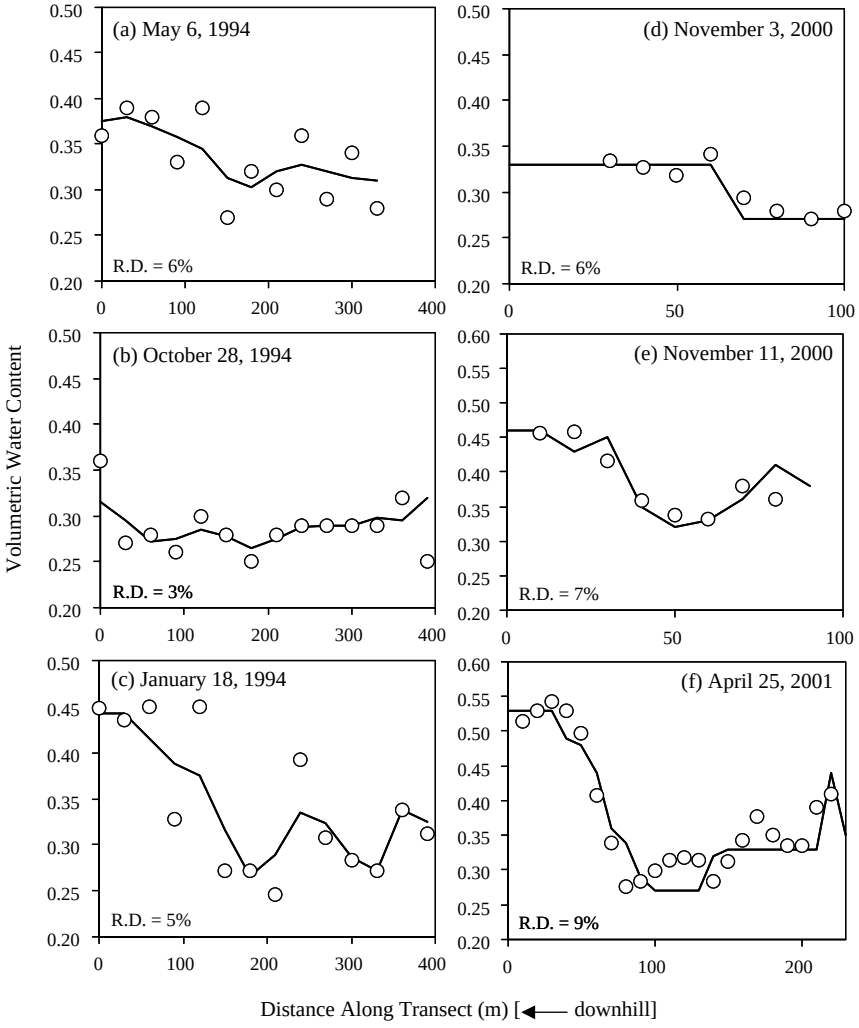

Fig. 5. Comparisons between SMR simulated soil moisture (lines) and measurements in the NYC watersheds for different months. (a)–(c) are from the Crowe Rd. Watershed (Frankenberger et al., 1999) and (d)–(f) are from Town Brook (Mehta et al., 2004). Measurements were taken along hillslope transects and the x-axis are distances along the transects with $x=0$ corresponding to the low end of the hills. Relative differences (R.D.) between measured and modeled soil moistures are shown in each graph. (R.D. = standard error/mean of observed).

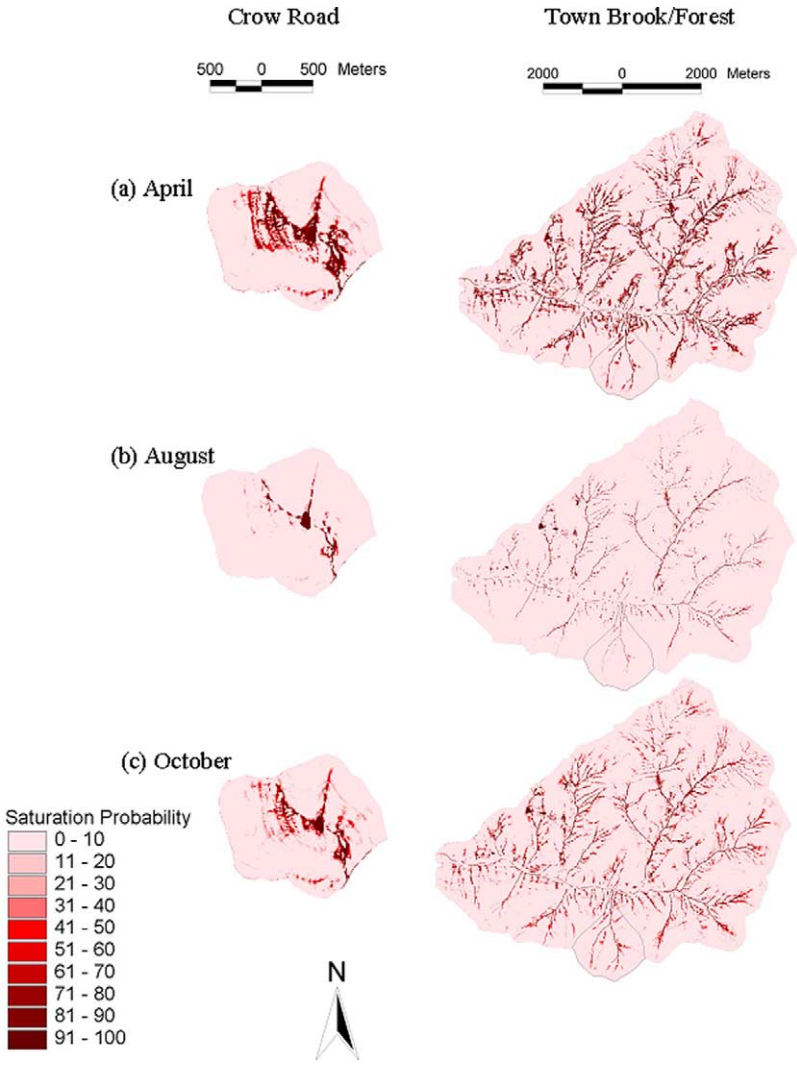

Fig. 6. Examples of saturation probability, P_{sat}, for a spring month, (a) April, a summer month, (b) August, and a fall month, (c) October. Results are shown for all three modeled watersheds. Darker color indicates higher P_{sat}.

λ_o and λ_{100}, respectively. For $\lambda_o < \lambda < \lambda_{100}$, a linear relationship between P_{sat} and λ was good, R^2 ranged between 0.89 and 1.00. Notice that λ_o shifts from roughly 8 in April to 10 in August and back to $\sim$8 in October (Fig. 7); in physical terms, all areas with $\lambda < 8$ have very low probabilities of generating saturation excess runoff ($P_{sat} < 5\%$) in the spring and fall and in the summer these low risk areas encompass all areas with $\lambda < 10$. While there is an easily recognized, well-behaved relationship for the average P_{sat} for different λ (symbols in Fig. 7), there is some variability as indicated by the dashed 25th and 75th percentile lines (Fig. 7). Some of this variability is expected because the proxy parameter λ is unlikely to capture all the complex spatial variability. Some variability, especially for the high λ, is due to the fact that SMR does not explicitly model the near-stream deep groundwater. As a result, in some river and riparian areas, SMR under-predicts P_{sat} during the summer and fall months because the model cannot saturate the relatively deep depositional soils in the river bottoms with upslope interflow, i.e. deeper groundwater maintains the water table near some parts of the stream. Evidence of this weakness in SMR can be seen in the discontinuously simulated stream for August (Fig. 6). Interestingly, in these areas the assumption that $\lambda > \sim 13$ corresponds to a perpetually saturated area is probably more realistic than the SMR predicted P_{sat} We are currently exploring unbiased approaches to parsimoniously correcting this problem in SMR, although it does not substantially influence the results here because the problem is restricted to streambeds, which are already protected.

As expected, the average P_{sat}–λ relationships among the watersheds were very similar due to relatively similar geology and climate among the three watersheds (Fig. 8). Thus, we can use a single set of monthly P_{sat}–λ relationships throughout for all three watersheds (Fig. 8), and presumably throughout the region. Qualitatively, the general patterns of hydrological sensitivity (dark areas in Fig. 8) are similar to those of high P_{sat} (Fig. 6), with larger hydrologically

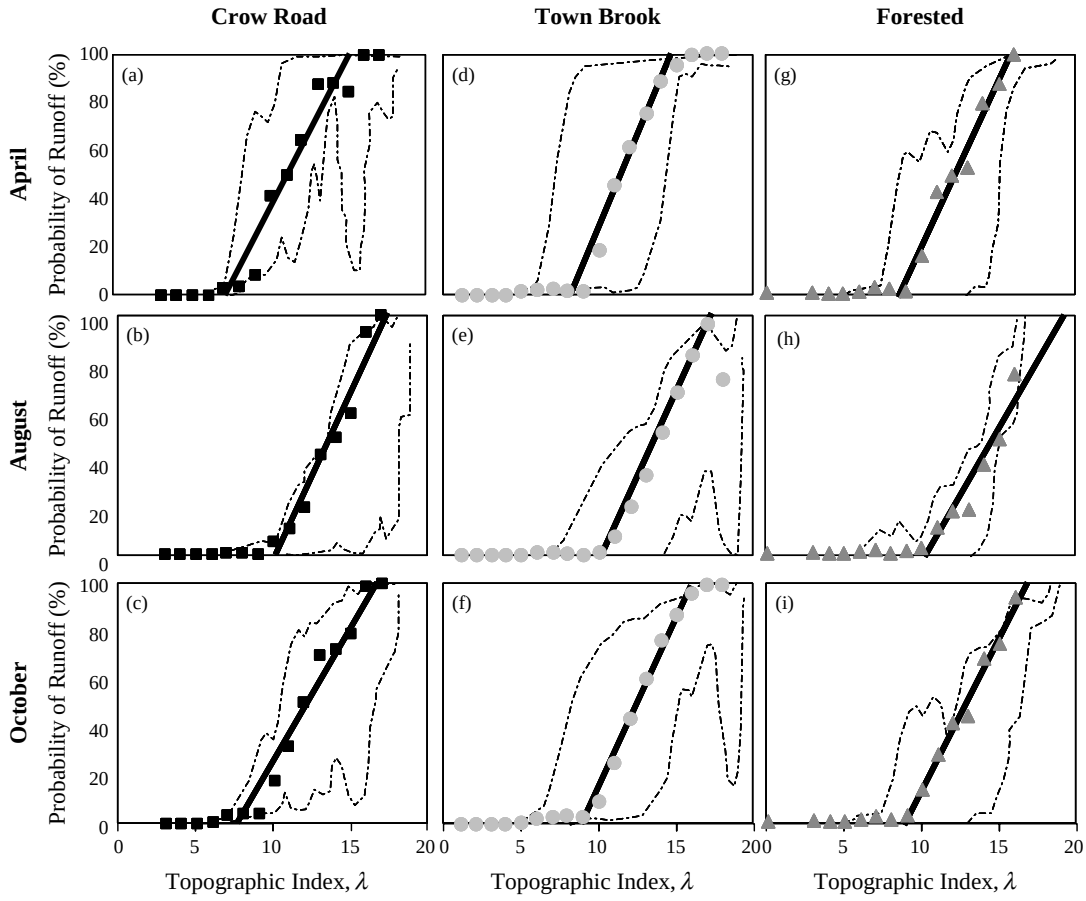

Fig. 7. P_{sat}–λ relationships for the (a–c) Crowe Road, (d–f) Town Brook, and (g–i) Forested watersheds for (a, d, g) April, (b, e, h) August, and (c, f, i) October. The symbols are the average P_{sat} for corresponding λs. The dashed lines correspond to the 25th and 75th percentiles, i.e. half the P_{sat} values for any given topographic index lie between the two dashed lines. The percentile lines determined using built-in commands in GRI Graphing Language.

sensitive, i.e. runoff producing, areas in April and October than in the relatively dry month of August. Note also that even between the 'wet' months of April and October there are potentially significant differences in the extent of HSAs. Table 1 shows the $P_{sat}(\lambda)$ functions for all 12 months. Interestingly, the variability between watersheds is less than the intra-watershed variability (dashed lines in Fig. 7). The composite or regional P_{sat}–λ trend for the range $\lambda_o < \lambda < \lambda_{100}$ was nearly as good as for the individual watersheds, $R^2 =$ 0.86–0.95 (Table 1).

For April and August we were able to compare our P_{sat}–λ relationships to field measurements of P_{sat} determined via the matrix of piezometers in part of Town Brook (filled circles, Fig. 8). For April, the P_{sat}–λ relationship determined by SMR was similar to the observed relationship (Fig. 8a). For August, we observed substantially higher P_{sat} than our model predicted (Fig. 8b). These differences are readily attributable to the 2004 rainfall patterns; March 2004 rainfall (6.1 cm) was nearly equal to the 30-year normal rainfall (6.4 cm) whereas August 2004 (19.3 cm) was over twice the normal (8.6 cm). The comparison of our model to field measurements for a specific year emphasizes the fact that our P_{sat}–λ relationships provide average risks and that actual relationships will shift with specific weather patterns.

4.3. Stream proximity results

There was are clear trends of generally decreasing saturation probability, P_{sat}, with increasing distance from the stream, D_s, for all three test watersheds but it is obvious that there was substantial variability among the three watersheds (Fig. 9). For example, in April average $P_{sat} \approx 5\%$ for the Crow Road, Town Brook, and Forested watersheds corresponded to D_s of about 30, 75, and 20 m, respectively (Fig. 9). Unlike the P_{sat}–λ relationships (Fig. 7), it was not feasible to make similar estimates of intra-watershed variability between P_{sat} and D_s because the distribution of P_{sat} for most D_s values was not continuous but rather clumped and in almost all D_s zones P_{sat} ranged from 0 to 100%. The problematic nature of using D_s as a proxy for hydrological sensitivity is also evident in the measured P_{sat} results (filled circles, Fig. 9a,b), which show a less obvious or intuitively systematic trend than the modeled average watershed-wide results. Logarithmic and power

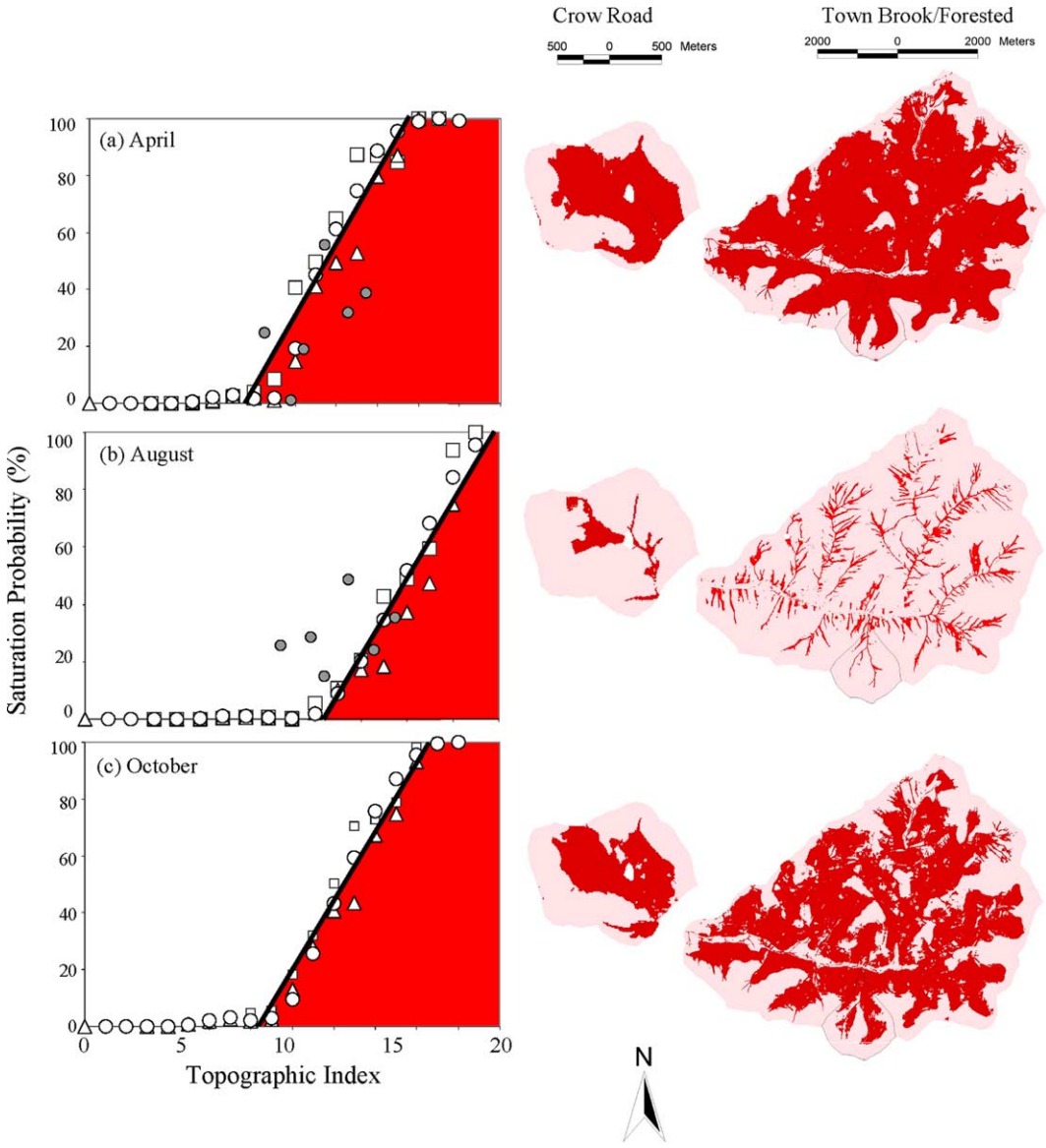

Fig. 8. The composite P_{sat}–λ relationships using the data from all three watersheds (open symbols) and the corresponding maps of HSA distributions in the watersheds based on the composite relationships for (a) April, (b) August, and (c) October. The shaded areas in the maps correspond to areas with $P_{sat} > 5\%$, i.e. indicated by the shaded area in the graphs. Squares = Crow Road, triangles = forested watershed, open circles = Town Brook, and filled circles = field measurements in Town Brook [(a) and (b) only].

function best described the P_{sat}–D_s relationships with correlation coefficients, R^2, between 0.55 and 0.66 over all months (Table 2), which were relatively poor compared to the P_{sat}–λ relationships shown in Table 1.

5. Discussion

As expected, the topographic index, λ, was a more consistent and reliable indicator of hydrological sensitivity than stream proximity, D_s. This result was expected simply because of the copious research that has shown good agreement between topographic indices and saturated areas (e.g. Beven and Kirkby, 1979; Walter et al., 2002; Gunter et al., 2004; Ibbit and Woods, 2004) and because topography is a primary hydrological driver in SMR. Recall that the purpose of this exercise was to assign quantifiable risks of hydrological sensitivity to simple proxy-parameter, not to compare 'models' per se. Because all three watersheds showed very similar monthly relationships between P_{sat} and λ, it is plausible that the relationships presented here are reliable for surrounding watersheds with similar geology, topography, and weather, i.e. probably throughout Delaware Co.

Although we anticipated the good agreement between λ and P_{sat}, there was considerable interest in the stream proximity approach because, as mentioned earlier, it is extremely easy to measure. The problem with using D_s as an

Table 1
Summary of the monthly composite or regional correlation between P_{sat} and λ

Month	Topographic index boundary values		$P_{sat}(\lambda)$ For $\lambda_o < \lambda < \lambda_{100}$	R^2 [a]
	λ_o [b]	λ_{100} [c]		
January	8.0	15.2	$P_{sat} = 13.9\lambda - 111.8$	0.87
February	7.9	15.5	$P_{sat} = 13.1\lambda - 103.3$	0.88
March	8.0	15.3	$P_{sat} = 13.6\lambda - 108.5$	0.86
April	7.6	15.5	$P_{sat} = 12.7\lambda - 96.3$	0.91
May	8.5	16.2	$P_{sat} = 13.0\lambda - 110.5$	0.95
June	9.7	17.0	$P_{sat} = 13.7\lambda - 133.3$	0.94
July	10.3	17.8	$P_{sat} = 13.4\lambda - 137.9$	0.91
August	10.3	17.7	$P_{sat} = 13.4\lambda - 137.5$	0.93
September	9.9	17.2	$P_{sat} = 13.8\lambda - 137.2$	0.94
October	8.4	16.7	$P_{sat} = 12.0\lambda - 100.2$	0.95
November	7.9	15.4	$P_{sat} = 13.3\lambda - 105.0$	0.92
December	7.7	15.0	$P_{sat} = 13.7\lambda - 105.6$	0.89

[a] Correlation coefficients for the relationship in the range of $\lambda_o < \lambda ?? \lambda_{100}$.
[b] $P_{sat} = 0\%$ for $\lambda < \lambda_o$.
[c] $P_{sat} = 100\%$ for $\lambda > \lambda_{100}$.

indicator of hydrological sensitivity can be readily observed in the Crow Road watershed; Fig. 10a shows two areas, (A) and (B), located the same distance from the stream with significantly different values of P_{sat}, or different risks of generating overland flow. The topographic index more accurately characterizes the differences in P_{sat} between these two locations (Fig. 10b) than simple stream proximity (Fig. 10c). This example suggests that rather than defining 'riparian buffer areas' as a setback distance from a stream, one might consider protecting riparian areas in order to restrict contaminant loading on these near-stream areas that are likely to produce overland flow. This change in conceptual basis for riparian 'buffers' is probably more justifiable than the current belief that they provide some sort of 'runoff filtering or remediation,' especially with respect to dissolved contaminants.

We anticipate that the most immediate use for our HSA tool will be to aid in identifying critical source areas, CSAs, for which water quality protection efforts could be focused. For example, using the HSA relationships we determined for April, August, and October (Table 1) we can make HSA maps assuming, say, all area with $P_{sat} > 5\%$ are hydrologically sensitive (dark areas in Fig. 11). Overlaying field boundaries on the HSA map, the places where HSAs overlap field areas can be readily identified as CSAs (Fig. 11). Walter et al. (2000, 2001) proposed avoiding placement potential pollutants, such as animal manures or pesticides, on the HSAs, noting that some fields that are hydrologically sensitive in April and October are not in August, thus, at least in the case of animal manures, application could be rotated to avoid HSAs. Considering a dynamic pollution risk metric like the VSA-based concept presented here potentially lessens land use restrictions on landowners relative to static land classification schemes like that used to determine highly erodable lands. Other strategies using our 'HSA tool' might also be developed. For example, fields could be prioritized by their degree of

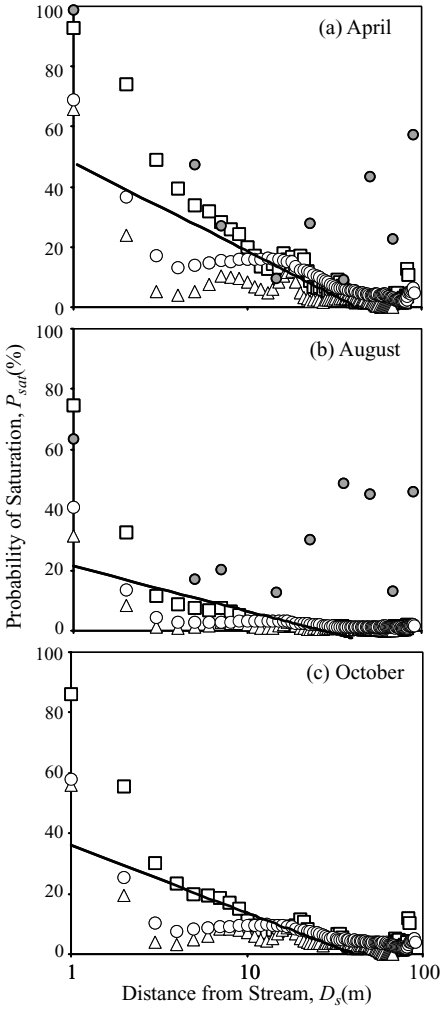

Fig. 9. D_s–P_{sat} relationships for (a) April, (b) August, (c) and October for all three watersheds (open symbols). The lines show the best-fit relationships for the combined data (see Table 2 for specific equations). Squares = Crow Road, triangles = forested watershed, open circles = Town Brook, and filled circles = field measurements in Town Brook [(a) and (b) only].

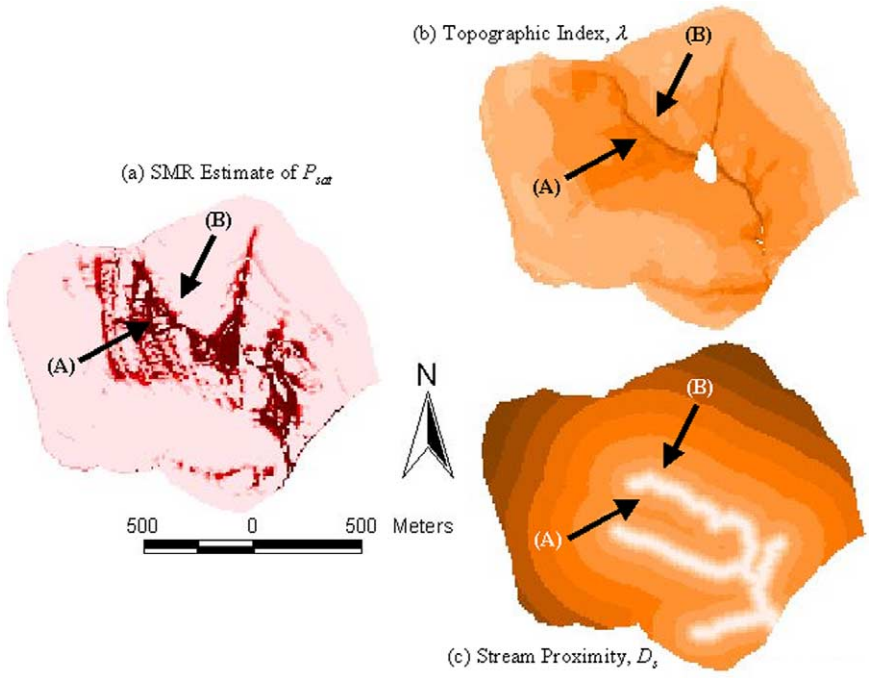

Fig. 10. Illustration of how the (b) λ and (c) D_s correspond to (a) our best estimate P_{sat} as determined with the SMR model. Locations (A) and (B) are the same distance from the stream. Color scales for (a), (b), and (c) are the same as for Figs. 5, 3, and 4, respectively.

hydrological sensitivity in ways that crops requiring the most pesticides are planted in fields with the lowest extent or frequency of HSAs. The authors encourage these approaches in conjunction with improvements to other, non-hydrological management practices. For example, revised nutrient management plan strategies that focus on substantially reducing nutrient importation to a watershed would be another valuable water quality tool, especially for long-term improvements. It should also be noted that incorporating tile drainage to reduce surface saturation is not a viable solution because, as shown by Geohring et al. (2001), this simply reroutes overland flow into the tile with little attenuation in pollutant loading, even for strongly sorbed constituents like phosphorus.

Although this study focused on HSAs that arise from VSA hydrology, it is little effort to include impervious, or low permeability areas, into the definition of HSA, and develop maps, or GIS coverages, that reflect this added, Hortonian aspect of pollutant transport risk. Indeed, this is being included in the current development of an Internet HSA tool that will be available to planners and water quality professionals that do not have substantial GIS expertise. The immediate web-based GIS-tool, due out by early May 2005, will only be applicable for Delaware County, New York because we are not confident that the relationships presented here are applicable to a wider area, mostly because of differences in weather. The tool will be accessible through the following URL: http://www.bee.cornell.edu/swlab/SoilWaterWeb/.

There are currently no plans to develop a similar tool for the stream proximity approach to identifying HSAs but rather expect that this method, if used rationally, can help locate HSAs in the field when no computers are available. Work is currently underway to modify the concepts in this paper for the entire northeastern U.S.

We are currently investigating ways to identify HSAs over larger regions by including rainfall information in our 'topographic index.' We are specifically considering an index of the form:

$$\lambda = \ln\left(\frac{aR}{\tan(\beta)K_s D}\right) \quad (2)$$

where R is some measure of rainfall (m d^{-1}), e.g. annual average, net monthly precipitation, etc; notice that λ is dimensionless when presented this way.

6. Conclusion

This study presented one way of incorporating up-to-date hydrological science with water quality management. Specifically, we developed a simple way of predicting hydrological sensitivity associated with variable source area hydrology. Because there is a clear, regionally consistent relationship between the topographic index, λ, and the probability of saturation, P_{sat}, with strong correlation throughout the year, we showed that λ could be used to identify and quantify the risk of saturation excess runoff. There is also a correlation between 'distance from a stream,' D_s, and P_{sat}, but the relationship is not as strong as for λ nor is it consistent among watersheds so it is considerably less reliable for predicting HSAs. The topographic index can be calculated using a GIS from readily

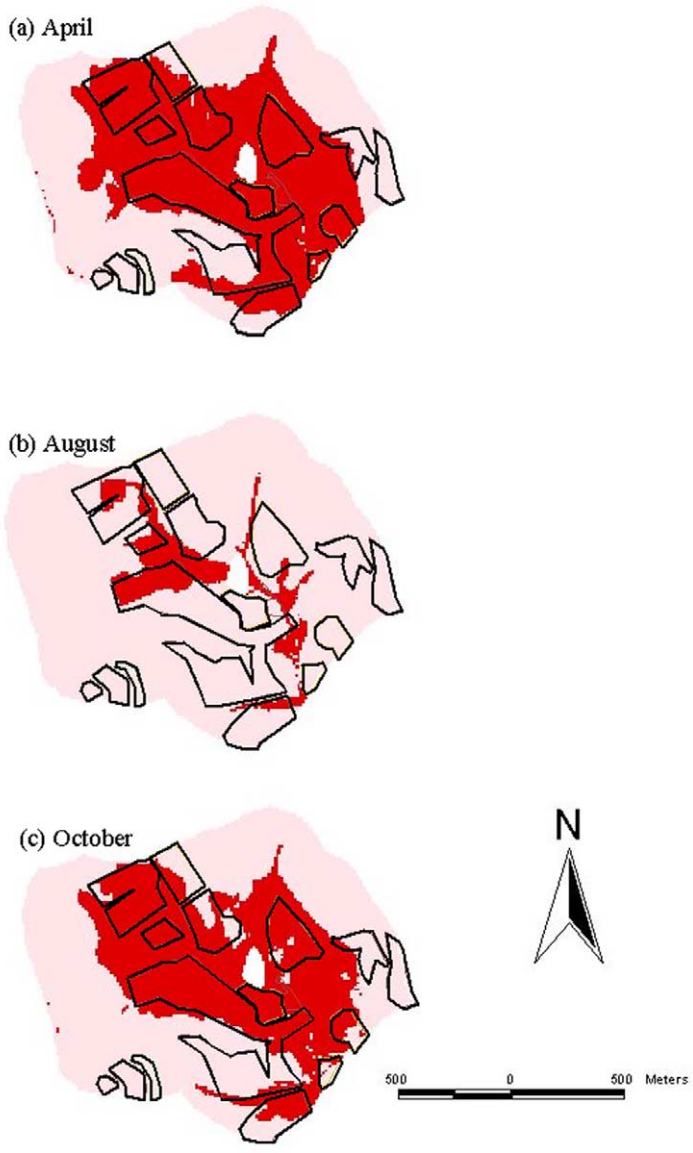

Fig. 11. HSA maps (λ corresponding to $P_{sat} > 5\%$) for the Crow Road watershed with field outlines shown for April (a), August (b), and October (c). This simple visual tool can be used to determine CSAs, i.e. the areas where fields overlay HSAs.

available geospatial data, specifically, topographic and soils data. The relationships presented here can be used to determine the location and associated risk of HSAs, and then overlaid with land use patterns to identify CSAs, or perhaps a better descriptor is critical management areas, CMAs.

A VSA web page is being developed which covers an introduction to the VSA concept and the relationship to environmental planning. The results and tools from this study along with continuing research in the area of VSA hydrology are or will be published as a part of this web site. The link for the site is: http://www.bee.cornell.edu/swlab/vsa/index.htm.

References

Ambroise, B., Beven, K., Freer, J., 1996. Toward a generalization of the TOPMODEL concepts: topographic indices of hydrological similarity. Water Resources Research 32 (7), 2135–2145.

Arnold, J.G., Allen, P.M., Bernhardt, G., 1983. A comprehensive surface-groundwater flow model. Journal of Hydrology 142, 47–69.

Bernier, P.Y., 1985. Variable source areas and storm flow generation: an update of the concept and a simulation effort. Journal of Hydrology 79, 195–213.

Beven, K.J., 1989. Changing ideas in hydrology: the case of physically-based models. Journal of Hydrology 105, 157–172.

Beven, K.J., 2000. Rainfall-Runoff Modeling, The Primer. Wiley, England.

Beven, K.J., Kirkby, M.J., 1979. A physically based, variable contributing area model of basin hydrology. Hydrological Science Bulletin 24, 43–69.

Brannan, K.M., Mostaghimi, S., McClellan, P.W., Inamdar, S., 2000. Animal waste BMP impacts on sediment and nutrient losses in runoff from the Owl run watershed. Transactions of the ASAE 43 (5), 1155–1166.

Dunne T., 1970. Runoff production in humid areas. U.S. Department of Agriculture Publication ARS-41-160. 108 pp.

Dunne, T., Black, R.D., 1970. Partial area contributions to storm runoff in a small New England watershed. Water Resources Research 6, 1296–1311.

Dunne, T., Leopold, L.B., 1878. Water in Environmental Planning. W.H. Freeman and Company, New York.

Dunne, T., Moore, T.R., Taylor, C.H., 1975. Recognition and prediction of runoff-producing zones in humid regions. Hydrological Sciences Bulletin 20 (3), 305–327.

Frankenberger, J.R., Brooks, E.S., Walter, M.T., Walter, M.F., Steenhuis, T.S., 1999. A GIS-based variable source area model. Hydrological Processes 13 (6), 805–822.

Gburek, W.D., Sharpley, A.N., 1998. Hydrologic controls on phosphorus loss from upland agricultural watersheds. Journal of Environmental QualitySharpley 27, 267–277.

Gburek, W.J., Drungil, C.C., Srinivasan, M.S., Needelman, B.A., Woodward, D.E., 2002. Variable-source-area controls on phosphorus transport: bridging the gap between research and design. Journal of Soil and Water Conservation 57 (6), 534–543.

Geohring, L.D., McHugh, O.V., Walter, M.T., Steenhuis, T.S., Akhtar, M. S., Walter, T.F., 2001. Phosphorus transport into subsurface drains by macropores after manure applications: Implications for best manure management practices. Soil Science 166 (12), 896–909.

Grayson, R.B., Moore, I.D., McMahon, T.A., 1992. Physically based hydrologic modeling 2. Is the concept realistic? Water Resources Research 28, 2659–2666.

Gunter, A., Seibert, J., Uhlenbrook, S., 2004. Modeling spatial patterns of saturated areas: an evaluation of different terrain indices. Water Resources Research 40, W0114.

Haith, D.A., Shoemaker, L.L., 1987. Generalized watershed loading functions for strem-flow nutrients. Water Resources Research 23 (3), 471–478.

Hewlett, J.D., Hibbert, A.R., 1967. Factors affecting the response of small watersheds to precipitation in humid regions. Forest Hydrology, 275–290.

Hewlett, J.D., Nutter, W.L., 1970. The varying source area of streamflow from upland basins, Proceedings of the Symposium on Interdisciplinary Aspects of Watershed Management. Held in Bozeman, MT. ASCE, New York pp. 65–83.

Hively W.D., 2004. Data preparation for distributed hydrological modeling of runoff production and dissolved phosphorus loading. In Hively W.D., Phosphorus loading from a monitored dairy farm landscape. PhD Thesis. Cornell University, Ithaca, NY.

Holko, L., Lepisto, A., 1997. Modelling the hydrological behaviour of a mountain catchment using TOPMODEL. Journal of Hydrology 196 (1–4), 361–377.

Horton, R.E., 1933. The role of infiltration in the hydrologic cycle. Transactions American Geophysical Union 14, 446–460.

Horton, R.E., 1940. An approach toward a physical interpretation of infiltration capacity. Soil Science Society of America Proceedings 4, 399–417.

Hursh, C.R., 1944. Report of the subcommittee on subsurface flow. Transactions of the American Geophysical Union 25, 743–746.

Ibbitt, R., Woods, R., 2004. Re-scaling the topographic index to improve the representation of physical processes in catchment models. Journal of Hydrology 293, 205–218.

Inamdar, S.P., Mostaghimi, S., McClellan, P.W., Brannan, K.M., 2001. BMP impacts on sediment and nutrient yields from an agricultural watershed in the coastal plain region. Transactions of the ASAE 44 (5), 1191–1200.

Kuo W.L., Longabucco P., Rafferty M.R., Boll J., Steenhuis T.S., 1996. An integrated GIS-based model for soil water and nitrogen dynamics in a New York City watershed. Proceedings of the American Water Resources Association Symposium on Watershed Restoration Management. Syracuse, NY, 1996, pp. 17–26.

Lyon, S.W., Gérard-Marcant, P., Walter, M.T., Steenhuis, T.S., 2004. Using a topographic index to distribute variable source area runoff predicted with the SCS-Curve Number equation. Hydrological Processes 18 (15), 2757–2771.

Lyon, S.W, Lembo A.J., Walter M.T., Steenhuis T.S., 2005. Defining probability of saturation with indicator kriging on hard and soft data. Advances in Water Resources (in press).

Mehta, V.K., Walter, M.T., Brooks, E.S., Steenhuis, T.S., Walter, M.F., Johnson, M., Boll, J., thongs, D., 2004. Application of SMR to modeling watersheds in the Catskill mountains. Environmental Modeling and Assessment 9, 77–89.

O'Loughlin, E.M., 1986. Prediction of surface saturation zones in natural catchments by topographic analysis. Water Resources Research 22, 794–804.

Quinn, P., Beven, K., Chevallier, P., Planchon, O., 1991. The prediction of hillslope flow paths for distributed hydrological modeling using digital terrain models. Hydrological Process 5, 59–80.

Rallison, R.K., 1980. Origin and evolution of the SCS runoff equation. In *Proceedings of Symposium on Watershed Management*, 21–23 July, Boise, ID. American Society of Civil Engineers: New York, NY; 912–924.

Rossing J.M., Walter M.F., 1995. Hydrologically-based identification of critical areas for water quality protection in the New York City watershed. ASAE Paper No. 952580, Presented at ASAE Annual International Meeting, Chicago, IL. 10 pp.

Segars W.I. 1997. Overview of federal and state regulations affecting livestock and poultry operations. Southeastern sustainable annual waste management workshop proceeding, Rural Development Center, Tifton, GA.

Sivapalan, M., Beven, K.J., Woods, E.F., 1987. On hydrological similarity 2. A scaled model of storm runoff predictions. Water Resources Research 23, 2266–2278.

SWL website. www.bee.cornell.edu/swlab/SoilWaterWeb/. Department of Biological and Environmental Engineering. Cornell University, Ithaca, NY.

Tollner, E.W., 2002. Natural Resources Engineering. Iowa State Press, Iowa pp. 105–106.

U.S. Army CERL, 1991. GRASS 4.1 Users' Manual. Construction Research Laboratory, Champaign, IL.

USDA-SCS. 1972. Hydrology Sect. 4, Soil Conservation Service National Engineering Handbook. U.S. Department of Agriculture, Soil Conservation Service, Washington, DC.

USDA-SCS. 1986. Urban hydrology for small watersheds. Technical Release 55. U.S. Department of Agriculture, Soil Conservation Service, Washington, DC.

Walter, M.F., Steenhuis, T.S., Haith, D.A., 1979. Nonpoint source pollution control by soil and water conservation practices. Transactions of the ASAE 22 (5), 834–840.

Walter, M.T., Walter, M.F., Brooks, E.S., Steenhuis, T.S., Boll, J., Weiler, K.R., 2000. Hydologically sensitive areas: variable source area hydrology implications for water quality risk assessment Journal of Soil and Water Conservation. 3 277–284www.bee.cornell.edu/faculty/walter/HSAhome.htm.

Walter, M.T., Brooks, E.S., Walter, M.F., Steenhuis, T.S., Scott, C.A., Boll, J., 2001. Evaluation of soluble phosphorus transport from manure-applied fields under various spreading strategies. Journal of Soil and Water Conservation 56 (4), 329–336.

Walter, M.T., Steenhuis, T.S., Mehta, V.K., Thongs, D., Zion, M., Schneiderman, E., 2002. Refined conceptualization of TOPMODEL for shallow subsurface flows. Hydrological Processes 16, 2014–2046.

Walter, M.T., Mehta, V.K., Marrone, A.M., Boll, J., Gérard-Merchant, P., Steenhuis, T.S., Walter, M.F., 2003. A simple estimation of the prevalence of Hortonian flow in New York City's watersheds. ASCE Journal of Hydrological Engineering 8 (4), 214–218.

Wigmosta, M.S., Vail, L.W., Lettenmaier, D.P., 1994. A distributed hydrology-vegetation model for complex terrain. Water Resources Research 3, 1665–1679.

Young, R.A., Onstad, C.A., Boesch, D.D., Anderson, W.P., 1989. AGNPS—a nonpoint-source pollution model for evaluating agricultural watersheds. Journal of Soil and Water Conservation 44 (2), 168–173.

Zollweg, J.A., W, J., 1996. SmoRMod—a GIS-integrated rainfall-runoff model. Transactions of the ASAE 39 (4), 1299–1307.